A New Synthetic Agent with Potent but Selective Cytotoxic Activity against Cancer

Wieslaw M. Cholody,[†] Teresa Kosakowska-Cholody,[†] Melinda G. Hollingshead,[‡] Humcha K. Hariprakasha,[†] and Christopher. J. Michejda*,[†]

Molecular Aspects of Drug Design, Structural Biophysics Laboratory, Center for Cancer Research, National Cancer Institute—Frederick, Frederick, Maryland 21702, and Developmental Therapeutics Program, National Cancer Institute—Frederick, Frederick, Maryland 21702

Received December 30, 2004

The synthesis of novel unsymmetrical bifunctional antitumor agents was accomplished by linking an imidazoacridone moiety to another polycyclic heteroaromatic moiety via linkers of various length and rigidity. These compounds bind to cellular DNA, but it is hypothesized that biological effects become manifested when the drug−DNA complexes interact with critical DNA binding proteins that are involved in repair and transcription. The most promising compound of the series, **4ad** (WMC79), consists of an imidazoacridone linked to a 3-nitronaphthalimide moiety via a 1,4-dipropanopiperazine linker. It was found to be potently, but selectively, cytotoxic against colon cancers (GI_{50} = 0.5 nM, LC_{50} = 32 nM) and leukemias (GI_{50} = 3.5 nM, LC_{50} = 33 nM). Compound **4ad**, which appears to be a candidate for further development as an anticancer drug, kills sensitive cells by induction of apoptosis. It also showed significant in vivo activity against HCT-116 colon cancer xenografts in nude mice. Other compounds in the series also exhibited antitumor properties, but they were significantly lower than that of **4ad**.

Introduction

Many clinically effective anticancer drugs, regardless of their primary cellular targets (see Table 1 in ref 1), kill tumor cells either by apoptosis in susceptible cell types[2−7] or by various nonapoptotic mechanisms including "slow cell death" or "aponecrosis".[8−10] Cytotoxic agents, however, frequently exhibit unspecific toxicities, which has limited enthusiasm for new cytotoxic agents. Nevertheless, the ability to *selectively* kill tumor cells remains a highly desirable property of potential new anticancer drugs.

Several years ago our laboratory reported on a new class of promising antitumor agents with remarkable selectivity against colon cancers — the bisimidazoacridones (BIAs).[11,12] Some of these compounds also exhibited potent and highly selective antiviral properties.[13] Structures **1** and **2** are typical BIAs, where **1**, called WMC-26, is a potently cytostatic antitumor compound that targets the GI tract and leukemias,[11] while **2**, called temacrazine, is an anti-HIV drug that targets the transcription of the integrated viral genome.[13] These compounds were originally designed to be bisintercalating agents, and their molecular construction was based on previous findings about the structural requirements for bisintercalation.[14−18] However, we found that although BIAs did bind to DNA, the mode of binding did not involve bisintercalation.[11,19] Likewise, their biological mode of action was substantially different from that of ditercalinium, a structurally related compound that is a classical bisintercalator.[20]Two structural features are crucial for antitumor activity of BIAs: the presence of two aromatic ring systems and the properties of the linker that joins the aromatic moieties. Spectroscopic studies on the mode of binding of representative BIAs to various types of DNA[19,21] revealed that only one of the aromatic residues intercalates into DNA, while the other aromatic moiety and the linker reside in the minor groove. These conclusions were based on a combination of steady state and time-resolved fluorescence spectroscopy studies, which indicated that only one chromophore was intercalated to DNA and fluorescence anisotropy measurements showed that the entire molecule was associated with the DNA helix. The best model to account for this behavior involves the intercalation of one chromophore while the other, together with the linker, resides in the minor groove. This model was additionally supported by DNA melting experiments and gel shift studies.[19] These and other results led us to hypothesize that the unique biological properties of BIAs reflect a highly specific interaction with DNA that allows the BIA−DNA com-

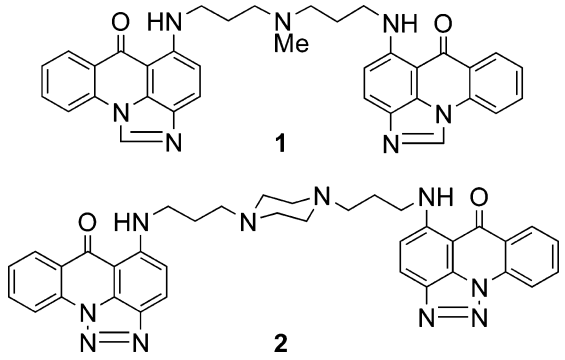

Figure 1. Structures of symmetrical bifunctional agents **1** and **2**.

* To whom correspondence should be submitted. Tel: 301-846-1216. Fax: 301-846-6231. E-mail: michejda@ncifcrf.gov.
† Molecular Aspects of Drug Design Section.
‡ Developmental Therapeutics Program.

10.1021/jm048946x
Published on Web 06/08/2005

Table 1. Cytotoxic Activity of New Agents against Selected Cancer Cell Lines

	tumor cell lines									
	HCT-116		A549		SK-MEL-2		HL-60		MCF-7	
compound	GI_{50}[a]	LC_{50}[b]	GI_{50}	LC_{50}	GI_{50}	LC_{50}	GI_{50}	LC_{50}	GI_{50}	LC_{50}
4ac	8	220	25	500	150	>1000	120	500	50	>1000
4ad	0.5	32	0.6	35	4	60	3.5	33	3.2	>1000
5ad	2.2	80	2.5	100	15	750	5	450	32	>1000
6	3.8	>1000	8	>1000	300	>1000	400	>1000	400	>1000
mitonafide	250	>1000	65	800	150	700	45	400	245	>1000

[a] GI_{50}: concentration of drug (nM) resulting in inhibition of cell growth to 50% of controls. [b] LC_{50}: concentration of drug (nM) required to reduce by 50% the initial cell number. The GI_{50} and LC_{50} values are the average of at least three independent determinations; the coefficients of variation were between 8 and 20%.

plex to interact with a critical DNA binding protein. The symmetrical BIAs, for example, are extremely potent inhibitors of HIV-1 integrase in a biochemical assay, where they interfere with 3′-processing and the strand transfer reaction. The biochemical results are best accounted for by the formation of a ternary complex of DNA, integrase and the BIA, which results in the inactivation of the enzyme.[13] It is clear that the two aromatic moieties play different roles, or in other words, the unsymmetrical DNA molecule induces asymmetry in the binding of the symmetric BIAs. Thus, the postulated model proposes that one of the aromatic moieties provides the means for docking the drug molecule to DNA by intercalation, while the second, together with the linker, interacts with a critical protein.

Since the role of the two aromatic moieties of symmetrical BIAs was different, it was interesting to examine the biological properties of molecules where the aromatic residues were in fact different. We expected that replacement of one imidazoacridone moiety with another planar ring system with a different tendency for intercalation to DNA could provide compounds with novel antitumor properties. To test this possibility, we exchanged one imidazoacridone chromophore of the BIAs with a variety of planar aromatic molecules. In this paper, we present the results of substitution of the imidazoacridone moiety with either a 1,8-naphthalimide or a 3-chloro-7-methoxyacridine moiety.

Chemistry

The general synthetic route to the new compounds is presented in Scheme 1. The starting monofunctional imidazoacridones **3ac** and **3ad** were described previously.[11,21] Compounds **3** were condensed with 3-nitro-1,8-naphthalic anhydride in *N*,*N*-dimethylformamide (DMF) to give compounds **4**. Compound **4ad** (which is commonly known as WMC79) was further transformed into **5ad** by reduction of the nitro group with stannous chloride. Compound **6** was synthesized by the reaction of **3ad** with 3-chloro-7-methoxy-9-phenoxyacridine in phenol.

The new compounds in their neutral state were completely insoluble in aqueous media. Consequently, they were transformed into tri(methanesulfonate) salts, which were sufficiently soluble in water and in dilute buffers for biological testing. Aqueous solutions were used for in vitro biological testing while 5% dextrose solutions were used for in vivo experiments. Other salts (hydrochlorides, hydrobromides, and trifluroacetates) were also prepared, but as was found with the symmetrical BIAs, the methanesulfonate salts appeared to have the most favorable properties for subsequent testing. The new compounds are highly fluorescent, as was the case for the symmetrical BIAs.[11,12] The fluorescent properties were very useful for studying cellular localization of the compounds and also for a variety of biophysical measurements. Spectroscopic experiments (Tarasov et al., unpublished results) show that **4ad** binds to DNA in an analogous manner to BIAs.[19] One aromatic moiety intercalates to DNA while the other, together with the linker, resides in the minor groove. However, unlike the symmetrical BIAs, **4ad** did not exhibit enhanced fluorescence in the presence of DNA.

All of the compounds reported in this paper are very stable in the solid state, especially in the methane-

Scheme 1[a]

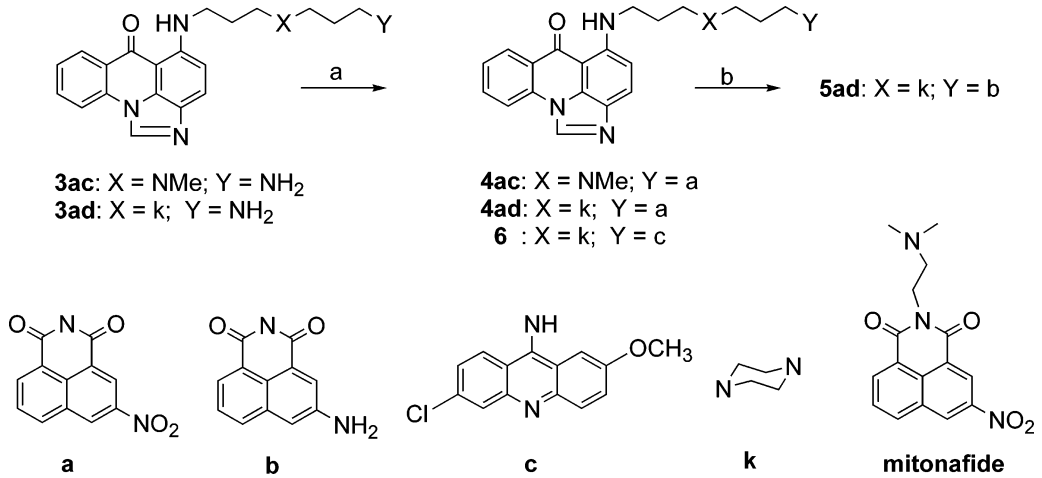

[a] Reagents and conditions: (a) **4**, 3-nitro-1,8-naphthalic anhydride, DMF, 80 °C; **6**, 3-chloro-7-methoxy-9-phenoxyacridine, phenol, 90 °C. (b) $SnCl_2$, HCl, AcOH, 60 °C.

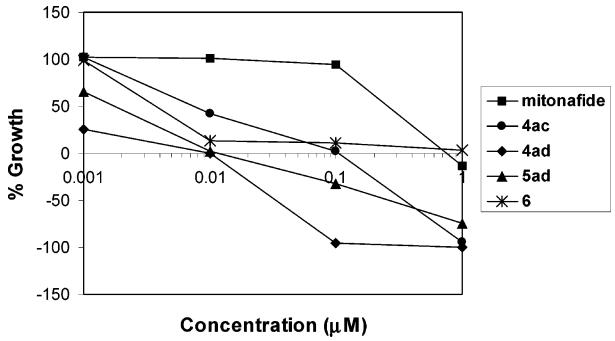

Figure 2. In vitro activity of new compounds against human colon cancer HCT-116 measured by a 5 day MTT assay as described in the Experimental Section. Similar experiments were run for other tumor cell lines, and the data were used to calculate the GI_{50} and LC_{50} values presented in Table 1. Values shown are means ± SD of at least of three independent experiments.

sulfonate form, but appear to suffer some photochemical degradation when dilute solutions are exposed to ambient light for prolonged periods of time. The compounds are also adsorbed onto glass and quartz surfaces, which affects the concentrations of dilute solutions significantly. Curiously, these solutions were not affected by polyethylene or polycarbonate surfaces; hence solutions in plastic containers could be stored without significant loss of material. All of the new compounds were subjected to biological testing.

Biological Results

Cytotoxicity. Initial evaluation of **4ac** (NSC 695941) and **4ad** (NSC 695942) in the standard National Cancer Institute (NCI) 60 human tumor cell line screen[22] showed a very high degree of growth inhibition (GI_{50}) but the capacity to produce cell killing (LC_{50}) was much less pronounced. The readings were made after a 48 h exposure of the cells to the chemicals. Consequently, we examined the effect of the compounds on several tumor cell lines utilizing the MTT assay[23] for cytotoxicity but extending the drug exposure time to 120 h. Figure 2 presents typical dose−response curves for HCT-116 colon tumor. The GI_{50} and LC_{50} values were determined from these and similar data for other tumor cell lines (Table 1). These results showed that **4ad**, which contains a 3-nitronaphthalimide chromophore and piperazine moiety in the linker, exhibited outstanding cytotoxic activity, with LC_{50} values (drug concentration required to reduce the initial cell number by 50% after 120 h) below 100 nM, against all of the cell lines except the breast cancer line MCF-7. Compound **4ac** a structural analogue with a somewhat shortened and more flexible linker was significantly less active at both the GI_{50} and LC_{50} levels. On the other hand, compound **6**, which contains the piperazine linker but has the naphthalimide chromophore replaced with a substituted acridine, resembled the original bisimidazoacridones and was devoid of the cell killing activity. Compound **5ad**, in which the nitro group was reduced to an amino group, was also cytotoxic but significantly less so than the oxidized nitro form. It is worth noting that mitonafide, a 3-nitronaphthalimide derivative (Scheme 1), which was tested in phase II clinical trials against colorectal cancer[24] and non-small-cell lung cancers,[25]

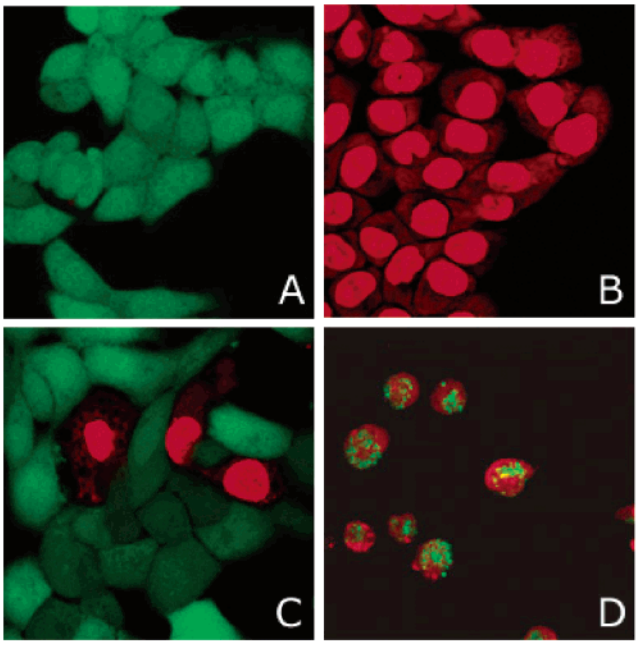

Figure 3. (A−D) The LIVE/DEAD two-color cell viability experiment: A, untreated colon tumor HCT-116 cells (live, negative control); B, cells treated with 70% ethanol for 30 min (dead, positive control); C and D, cells exposed to 100 nM **4ad** for 48 and 96 h, respectively. Both attached and floating cells were included in the assay.

showed only moderate cytotoxicity against two cell lines A549 and SK-MEL-2 cells and was not significantly active against the other lines tested.

LIVE/DEAD Viability/Cytotoxicity Assay. This two-color test clearly distinguishes between live cells with intracellular esterase activity (green fluorescence from the calcein produced by the enzymatic conversion of nonfluorescent calcein AM, Figure 3A) and dead cells with damaged membranes (red fluorescence from the ethidium dimer bound to the exposed cellular DNA, Figure 3B). This experiment confirmed the potent cytotoxicity of **4ad.** First, dead cells were detected after only 48 h of exposure to 100 nM of the drug, while 96 h of treatment caused the death of almost the entire population, as demonstrated by the red fluorescence from the ethidium dimer (Figure 3D).

DNA Fragmentation. The DNA from HL-60 cells treated with **4ad** and control untreated cells was extracted and analyzed by electrophoresis on agarose gels. Figure 4 shows that the genomic DNA of HL-60 cells treated with 100 nM **4ad** was severely fragmented at 72 and 96 h timepoints (lanes 4 and 5). Compound **4ad** causes the fragmentation of HL-60 DNA much more slowly than camptothecin, which induced maximal nucleosomal fragmentation of DNA after only 5 h of treatment (lane 6). The first signs of internucleosomal laddering were visible after 48 h of treatment in cells treated with **4ad** (lane 3).

DNA Staining. We used DAPI (4′,6-diamino-2-phenylindole), a DNA dye to examine morphological changes in the nuclei of untreated and drug-treated cells as well as to determine the percentage of apoptotic cells by fluorescence activated cell sorting (FACS) analysis. Treatment of HL-60 cells with 100 nM **4ad** results in the accumulation of cells in the sub-G_0/G_1 phase in a time-dependent manner. As shown in Figure 5, the popula

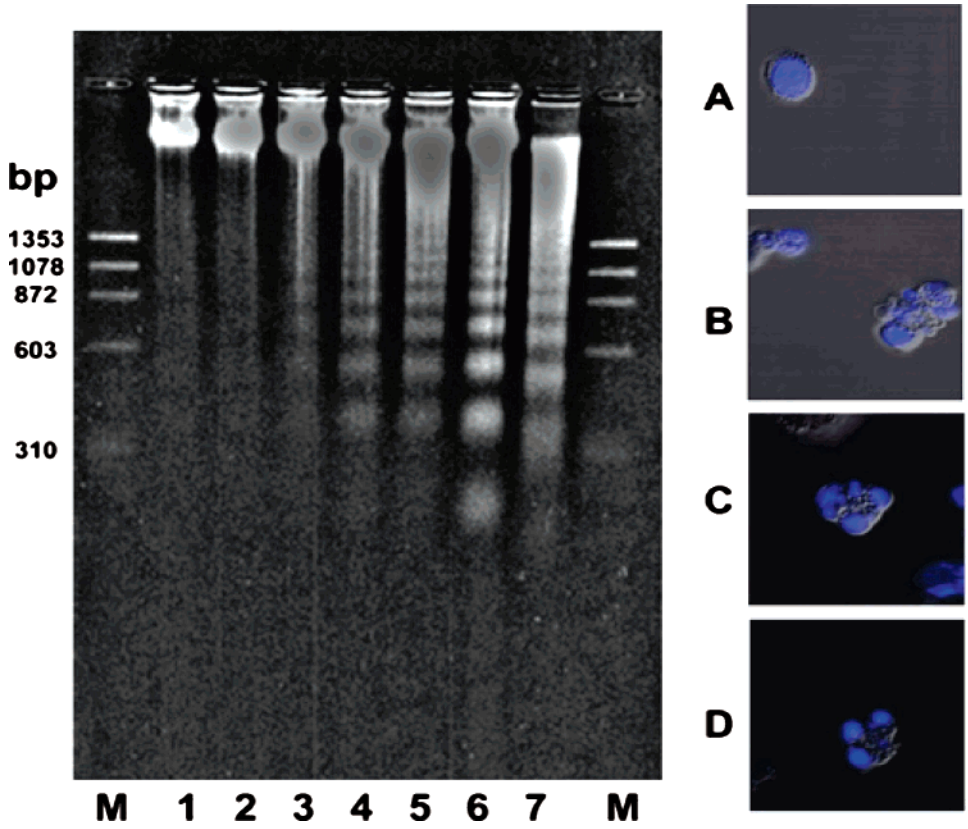

Figure 4. Internucleosomal DNA fragmentation and morphological changes induced by **4ad** in HL-60 cells**.** Agarose gel electrophoresis of DNA isolated from HL-60 untreated cells (lane 1), cells treated with 100 nM **4ad** for 24, 48, 72, and 96 h (lanes 2, 3, 4, and 5, respectively) or 100 nM camptothecin for 5 and 24 h (lanes 6 and 7). DNA was stained with ethidium bromide after electrophoresis on a 1.8% agarose gel and then visualized under UV light. Oligonucleosome-sized DNA fragmentation can be clearly seen in drug-treated cells after 72 and 96 h of treatment. Sizes of the molecular weight marker (M) are indicated to the left. DAPI staining shows morphological changes in the nuclei associated with DNA fragmentation: A, untreated cells and B, C, and D, cells exposed to 100 nM **4ad** for 48, 72, and 96 h, respectively. In the treated cells, the nuclei were fragmented, and this was visualized as apoptotic bodies.

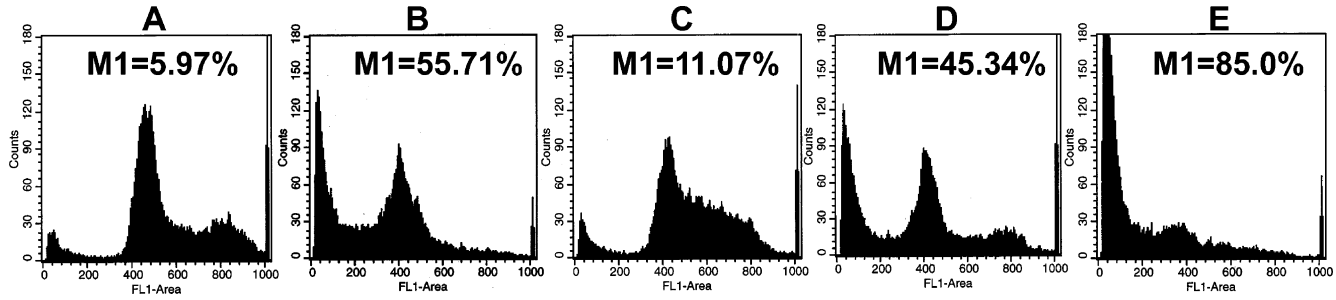

Figure 5. HL-60 nuclei stained with DAPI. HL-60 cells were incubated with and without **4ad** or camptothecin. The percent of apoptotic cells (M1) was determined by FACS after DAPI staining, as described in the Experimental Section: A, untreated cells; B, cells exposed to 100 nM camptothecin for 24 h; C, D, and E, cells treated with 100 nM **4ad** for 24, 72, and 96 h, respectively.

tion of apoptotic cells distinctly increased after 72 h of exposure to the drug (from 5.97% in untreated to 45.34% in drug-treated cells). These results are consistent with data obtained from the experiments described above.

Activation of Caspase-3. To examine the activity of the proapoptotic caspase-3, we used a specific fluorogenic caspase-3 substrate, Ac-DEVD-. Compound **4ad** caused a time-dependent increase in 7-amino-4-methylcoumarin (AMC) fluorescence that is consistent with the activation in caspase-3. As shown in Figure 6, caspase-3 activity was dramatically increased (sevenfold increase relative to untreated cells) in HCT-116 colon cancer after 48 h in response to 100 nM **4ad**. Only marginal activity was detected in the presence of the caspase-3 inhibitor (Ac-DEVD-CHO). In contrast, HL-60 cell lysates had a peak (10-fold) in enzyme activity after 72 h of treatment (data not shown).

In Vivo Studies. Compound **4ad** was administered intravenously (iv) to athymic mice (nu/nuNCr) implanted subcutaneously with HCT-116 human colon tumor xenografts. The drug was solubilized in 5% dextrose in water and given once every third day for a total of 5 doses. On this schedule, 40 mg/kg was toxic to 6 out of 10 animals while the 20 mg/kg and 10 mg/kg doses were well tolerated and showed significant inhibition of tumor growth. No significant dose response was evident from the data, which are presented in Figure 7.

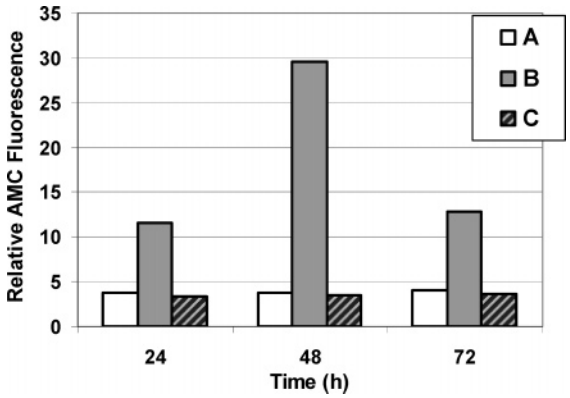

Figure 6. Time-dependent activity of caspase-3 in HCT-116 cells treated with **4ad**. Untreated and **4ad** treated HCT-116 cells were harvested at the indicated times. Cellular lysates were incubated with Ac-DEVD-AMC and caspase-3 substrate and analyzed for the presence of liberated AMC by spectrofluorometry (excitation at 380 nm, emission at 440 nm). Lysates from untreated cells were incubated with Ac- DEVD-AMC alone to determine the basal levels of apoptosis at each timepoint (A). Lysates from cells treated with 100 nM **4ad** were incubated with the substrate alone (B) and the substrate and the Ac-DEVD-CHO caspase-3 inhibitor (C). The highest level of caspase-3 activity was seen after 48 h of treatment with the drug.

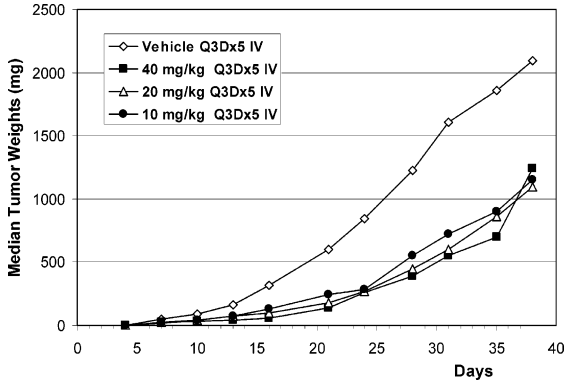

Figure 7. In vivo activity of **4ad** against human colon adenocarcinoma HCT-116 xenografts implanted subcutaneously in the flanks of athymic nude mice. Tumor cells were implanted 4 days prior to the initiation of treatment. The drug in 5% dextrose solution at the concentrations indicated or 5% dextrose control solution were administered iv 5 times every third day (Q3Dx5 schedule). The experiment was terminated at 38 days.

Discussion

The new unsymmetrical analogues of the BIAs, especially compound **4ad**, have substantially different biological behavior from their symmetrical progenitors. The symmetrical BIAs were purely cytostatic agents, exhibiting no cytotoxicity, even in concentrations as high as 10 μM. In contrast, the unsymmetrical compounds, except **6**, all showed significant cytotoxicity in the sensitive cell lines. Biophysical measurements of binding of the unsymmetrical agents to DNA revealed (Tarasov et al., unpublished data) that the mode of binding is similar to that of the one previously determined for the symmetrical BIAs,[19] which was described in the Introduction. We hypothesize that the difference in activity of the two series is the result of the differences in the ability of the DNA−drug complexes to "hijack" relevant proteins involved in DNA repair and/or transcription. Numerous, although circumstantial, lines of evidence suggest that the biological activities of BIAs, including the compounds presented in this paper, are the result of ternary complex formation involving the BIA, DNA, and a relevant protein. BIAs bind to DNA with K_D in the micromolar range,[19] but other experiments have shown that they do not bind to plasma proteins (Stinson, unpublished data), which suggest that binding to protein is weak. However, the biological activity of **4ad** is manifested at low nanomolar concentrations (see Table 1), several orders of magnitude lower than would be predicted from DNA binding data. This fact, together with the demonstration that ternary complexes can be seen in biochemical experiments, strongly suggests the formation of such complexes in cellular DNA and their involvement in the biological activity of the compounds.

As stated above, evaluation of **4ac** and **4ad** in the NCI 60 cell line screen showed very high, but selective, growth inhibition (GI_{50}) activity against some cancer types (colon, leukemia), while the level of cell killing (LC_{50} level) was much less pronounced.[22] This screening system is based on a short (48 h) exposure of tumor cells to drugs and frequently is too short to fully reveal the cytotoxic potency at physiologically relevant concentrations. Because induction of apoptosis in solid tumor cells often requires prolonged incubation, we used an extended drug exposure time (120 h) in a cytotoxicity assay. This was a more suitable means for evaluating the cell killing potency of the new chemicals. We selected five human tumor cell lines (colon tumor HCT-116, lung cancer A549, melanoma SK-MEL-2, breast cancer MCF-7, and leukemia HL-60) from the NCI panel and used them to test the target compounds in an MTT-based cytotoxicity assay. The strong cytotoxic effect detected at relatively low concentrations for **4ad** by MTT and LIVE/DEAD Viability/Cytotoxicity assays suggests that this agent may trigger apoptosis in sensitive cells. The occurrence of programmed cell death can be documented by many criteria, such as endonucleosomal DNA breakdown (DNA ladder), flow cytometric analysis of DNA content, induction of caspases, and morphological changes in dying cells among others. Usually, several different lines of evidence are required to establish apoptosis. We selected **4ad** as the most active compound in the series to evaluate the apoptosis-inducing properties. We used a concentration of 100 nM **4ad**, since that resulted in the complete killing of the cell lines under consideration. One hallmark of apoptosis is the demonstration of a "ladder" pattern in electrophoretic gels of nuclear DNA,[26] where a portion of nuclear DNA is fragmented to sizes equivalent to mono- or oligonucleosomes in cells that are undergoing apoptosis. We detected the formation of an apoptotic ladder in HL-60 leukemia cells (Figure 4) but not in HCT-116 colon tumor cells. The absence of DNA ladder in HCT-116 cells does not indicate the absence of apoptosis, since ladder formation occurs at a late stage of cell death and its presence is very dependent on the cellular model. This experiment also revealed that, in contrast to camptothecin, which induced apoptosis in HL-60 cells after only 5 h of treatment, **4ad** at an equivalent concentration required a much longer time (72 h). Apoptotic cell death was also detected by flow cytometric analysis of stained cell nuclei as well as by

the activation of caspase-3, a member of the interleukin 1β-converting enzyme family involved in the apoptotic cascade.[27] As presented in Figure 4, HL-60 cells treated with **4ad** show fragmentation of the nuclei. After 72 and 96 h of drug treatment, 45 and 85% of cells, respectively, were found to be undergoing apoptosis compared to 6% in the control cells (Figure 5). Caspase-3 is one of the key executioners of apoptosis, being responsible for the proteolytic activation of DNA-cleaving endonucleases.[28] Compound **4ad** was also able to induce caspase-3 activity in the colon line HCT-116 as well as in the leukemia line HL-60. Figure 6 presents the results of these experiments in HCT-116 cells. A noticeable elevation of caspase-3 activity over the background level was evident after 24 h of treatment, and the peak activity (more than 10 times the level of untreated cells) was observed after 48 h.

The in vitro activity of compound **4ad** was recapitulated in vivo. Figure 7 presents the results of an experiment wherein athymic (nu/nuNCr) mice with subcutaneous HCT-116 human colon cancer xenografts were treated iv with various concentrations of **4ad**. Preliminary experiments with intraperitoneal (ip) administration of **4ad** into tumor-bearing mice showed no antitumor activity, presumably because of first pass clearance of the drug in the liver (ip injected **4ad** had a plasma half-life of ~8 min). These results indicate that the drug inhibited the growth of the xenograft following 5 doses administered every third day. The absence of a dose response may be due to the toxicity of the drug. The highest dose (40 mg/kg) was toxic to 6 out of 10 animals, the intermediate dose (20 mg/kg) resulted in about a 10% body weight loss but no lethality, while the lowest dose (10 mg/kg) was well tolerated and just as effective as the higher doses. It is expected that additional in vivo experiments, with doses based on pharmacokinetic data, will allow us to determine an optimal dosing regimen. Nevertheless, the present data suggest that the drug is active in vivo and is relatively well tolerated.

Conclusion

The synthesis of unsymmetrical bifunctional agents, derived from the previously described BIAs, resulted in the discovery of a very potent but selective antitumor agent, **4ad**.This compound induced apoptosis in sensitive cells at low nanomolar concentrations in vitro. Preliminary data also indicated positive in vivo activity in a human colon cancer xenograft in nude mice. Compound **4ad** is a DNA-binding agent. We had previously shown that the symmetrical BIAs bind to DNA by intercalation and minor groove interaction. We believe that compounds such as **4ad** bind in a similar fashion. However, DNA binding is insufficient for biological activity. We hypothesize that compounds such as **4ad** exert their activity when the DNA−drug complex is able to "capture" a critical DNA-binding protein in a stable ternary complex. Ongoing studies will define the mechanistic basis for the potent, but selective, cytotoxicity of **4ad**.

Experimental Section

Chemical Synthesis. General. All of the commercial solvents and reagents were used without further purification. Column chromatography was performed on silica gel (Aldrich, 70-230 mesh). Melting points were determined on an electrothermal capillary melting point apparatus and are uncorrected. ^{1}H NMR spectra were recorded on a Varian VXR-S spectrometer operating at 500 MHz. Elemental analyses were performed by Atlantic Microlab, Inc., Norcross, GA.

Compounds **3ac** and **3ad** were prepared as described earlier[11,21] and were purified by reverse phase semipreparatory high-performance liquid chromatography on C-18 columns or by automated flash chromatography on silica gel.

General Procedure for the Preparation of 4. A mixture of 3-nitro-1,8-naphthalenedicarboxylic anhydride (0.001 mol) and the corresponding substituted 5-amino-2,10b-diazaaceanthrylen-6-one (**3**) was stirred at 80 °C in dimethylformamide (8 mL) until the reaction was completed (thin layer chromatography). The precipitated solid was filtered, washed with methanol, and dried and could be purified by column chromatography or by crystallization to yield the corresponding compound **4**.

Example: 2-(3-{4-[3-(6-Oxo-6*H*-2,10b-diaza-aceanthrylen-5-ylamino)-propyl]-piperazin-1-yl}-propyl)-5-nitro-2-aza-phenalene-1,3-dione (4ad). Orange crystals after crystallization from dimethylformamide−water: yield 82%; mp 227−230 °C; ^{1}H NMR ($CDCl_3$) 9.31 (d, 1H), 9.13 (d, 1H), 8.97 (t, 1H), 8.76 (m, 1H), 8.56 (m, 1H), 8.55 (s, 1H), 8.42 (m, 1H), 7.94 (m, 3H), 7.89 (m,1H), 7.54 (m, 1H), 6.78 (d, 1H), 4.29 (m, 2H), 3.45 (qt, 2H), 2.53 (t, 2H), 2.48 (br m, 4H), 2.39 (t, 2H), 2.34 (br m, 4H), 1.96 (m, 2H), 1.88 (m, 2H). Anal. ($C_{36}H_{33}N_7O_5$) C, H, N.

Example: 2-(3-{Methyl-[3-(6-oxo-6*H*-2,10b-diaza-aceanthrylen-5-ylamino)-propyl]-amino}-propyl)-5-nitro-2-aza-phenalene-1,3-dione (4ac). Purified by silica gel column chromatography using chloroform−methanol (8:1) mixture as the eluent: yield 74%; mp 218−221 °C; ^{1}H NMR ($CDCl_3$) 9.23 (d, 1H), 9.04 (d, 1H), 8.97 (t, 1H), 8.71 (m, 1H), 8.50 (s, 1H), 8.34 (m, 1H), 7.94 (d, 1H), 7.88 (m, 2H), 7.77 (m,1H), 7.49 (m, 1H), 6.77 (d, 1H), 4.27 (m, 2H), 3.50 (qt, 2H), 2.56 (t, 4H), 2.30 (s, 3H), 1.95 (m, 4H). Anal. ($C_{33}H_{28}N_6O_5$) C, H, N.

5-Amino-2-(3-{4-[3-(6-oxo-6*H*-2,10b-diaza-aceanthrylen-5-ylamino)propyl]-piperazin-1-yl}-propyl)-2-aza-phenalene-1,3-dione (5ad). Stannous chloride(1.52 g, 0.008 mol) dissolved in concentrated hydrochloric acid (5 mL) was added to a stirred solution of **4ad** (0.644 g, 0.001 mol) in glacial acetic acid (25 mL). The mixture was stirred at 60 °C for 2 h. After the mixture was cooled, acetone (50 mL) was added and it was stirred vigorously. Precipitate was collected by filtration, washed with acetone, and suspended in water (250 mL). The suspension was made basic (pH ~12) with sodium hydroxide, and the product was extracted with chloroform (5 × 50 mL). The crude product was chromatographed on silica gel column with chloroform−methanol (10:1) mixture containing 0.5% isopropylamine. The main fraction, after evaporation of solvents, yielded 0.550 g (89%) of yellow **5ad**: mp 219−222 °C; ^{1}H NMR ($CDCl_3$) 8.99 (m, 1H), 8.57 (m, 1H), 8.55 (s, 1H), 8.31 (m, 1H), 8.02 (d, 1H), 7.97 (m, 1H), 7.92 (m, 2H), 7.80 (m, 1H), 7.60 (m, 1H), 7.54 (d, 1H), 7.29 (m, 1H), 6.79 (d, 1H), 4.24 (m, 2H), 4.17 (s, 2H), 3.46 (qt, 2H), 2.51 (t, 2H), 2.48 (br m, 8H), 2.42 (t, 2H), 2.34 (br m, 4H), 1.93 (m, 2H), 1.87 (m, 2H). Anal. ($C_{36}H_{35}N_7O_3$)·$^1/_2H_2O$, C, H, N.

5-(3-{4-[3-(6-Chloro-2-methoxy-acridin-9-ylamino)-propyl]-piperazin-1-yl}-propylamino)-2,10b-diaza-aceanthrylen-6-one (6). A mixture of **3ad** (0.419 g, 0.001 mol), 6-chloro-2-methoxy-9-phenoxyacridine (0.364 g, 0.001 mol), and phenol (4 g) was heated at 90 °C for 12 h. After the mixture was cooled, 100 mL of chloroform was added and then poured into 100 mL of 1 N sodium hydroxide and crushed ice. The mixture was shaken, and the chloroform layer was separated, condensed, and chromatographed on a silica gel column with chloroform−methanol (5:1) mixture as an eluent. The major fraction gave 0.383 g (58%) of yellow **6**: mp 188−192 °C; ^{1}H NMR ($CDCl_3$) 9.05 (t, 1H), 8.55 (s, 1H), 8.54 (m, 1H), 8.15 (d, 1H), 8.04 (d,1H), 7.99 (d, 1H), 7.97 (d, 1H), 7.93 (d, 1H), 7.79 (m, 1H), 7.54 (m, 1H), 7.42 (m, 2H), 7.28 (m, 1H), 6.82 (d, 1H), 3.95 (s, 3H), 3.89 (m, 2H), 3.54 (m, 2H), 2.75 (t, 2H), 2.52 (m,

10H), 2.42 (t, 2H), 1.96 (m, 2H), 1.65 (m,2H). Anal. ($C_{38}H_{38}ClN_7O_2$)·$^1/_2H_2O$, C, H, N.

Biological Studies. Chemicals. All of the mammalian cell culture reagents, DNA Typing Grade Agarose, DNA Typing Grade TAE (Tris-Acetate/EDTA) buffer, ethidium bromide, Tris-HCl, and Trypan Blue Stain were purchased from GIBCO-BRL (Grand Island, NY). Tissue culture materials were purchased from Corning Inc. (Acton, MA). Ammonium acetate, DAPI′, dimethyl sulfoxide (DMSO), ethylenediaminetetraacetic acid (EDTA), gel loading solution, methanesulfonic acid, paraformaldehyde, proteinase K, RNase A, sodium chloride, and sodium dodecyl sulfate (SDS) were from Sigma-Aldrich (St. Louis, MO). Polaroid Polopan film was from the Polaroid Corporation (Cambridge, MA).

Cell Culture. Human colon carcinoma HCT-116, human melanoma SK-MEL-2, human small cell lung cancer A549, human leukemia HL-60, and human breast cancer MCF-7 cells were purchased from the American Type Culture Collection (Rockville, MD). HCT-116, SK-MEL-2, and A549 cells were grown in Dulbecco's modified Eagle's medium. HL-60 and MCF-7 cells were cultured in RPMI 1640 medium. Media were supplemented with 10% heat inactivated fetal bovine serum (FBS), 2 mM L-glutamine, 100 U/mL of penicillin, and 100 μg/mL of streptomycin. Cells were maintained in a humidified incubator at 37 °C in 5% CO_2 atmosphere.

Cytotoxicity Assay. Cells were seeded in six wells for each studied concentration into 96-well microtiter plates (100 μL of medium containing 1000−1500 cells per well) and were precultured for 1 day. Stock solutions (2.5 mM) of test compounds were prepared freshly by dissolving their free base forms in a distilled water−DMSO (50:50) mixture containing 3 equiv of methanesulfonic acid and further diluted with distilled water to the concentration of 500 μM. These solutions were used to prepare 2 μM of working solution and its 10-fold serial dilutions in appropriate media. An amount of 100 μL of drug containing medium or vehicle (control) was added to each well. The cytotoxicity was determined by the MTT-based, CellTiter96 Non-Radioactive Cell Proliferation Assay (Promega, Madison, WI) according to instructions provided by the supplier of the kit. While the drugs were added, assays were performed on extra reference plates to determine the cell population density at time 0 (T_0). After 120 h of incubation at 37 °C in a humidified atmosphere containing 5% CO_2, the assays were performed on test (T) and control (C) cells. The absorbance of the wells was determined at 544 nm by a FLUOstar/POLARstar Galaxy (BMG Labtechnologies GmbH) MicroplateReader. Cellular responses were calculated from the data as described previously:[23] $100 \times [(T - T_0)/(C - T_0)]$ for $T > T_0$ and $100 \times [(T - T_0)/T_0]$ for $T < T_0$.

LIVE/DEAD Viability/Cytotoxicity Assay. This experiment was performed according to the manufacturer's fluorescence microscopy protocol provided with the kit (Molecular Probes, Eugene, OR).

DNA Fragmentation. At specified times, untreated or drug-treated cells were collected by centrifugation at 2500*g* for 5 min. The resulting cell pellet (approximately 2×10^6 cells) was resuspended in a lysis buffer (0.5 M Tris, pH 8.0; 20 mM EDTA; 10 mM NaCl; 1% SDS). Lysates were transferred to Eppendorf tubes and incubated overnight at 37 °C with proteinase K (final concentration 0.5 mg/mL). The next day one-fourth of the volume of saturated NaCl solution (approximately 6 M) was added to the warm lysate. It was cooled in an ice slurry and centrifuged for 30 min at 500*g*. The supernatant was poured into a fresh tube and 0.2 vol of 11 M ammonium acetate, and 2 vol of cold 96% ethanol were added, mixed gently by inversion, and kept at −20 °C for several hours. After centrifugation at 14500*g* for 15 min at 4 °C, the pellet was washed twice in cold 70% ethanol, dried at room temperature, and dissolved in TE buffer (Tris-HCl pH 8.0, EDTA pH 8.0, NaCl), followed by treatment with DNase-free RNase A (100 μg/mL) for 3 h at 37 °C. DNA was quantitated using UV spectroscopy at an optical densityof 260 nm. DNA (10 μg) was mixed with loading buffer and transferred to the gel. Electrophoresis was then performed in 1.8% agarose gel in Tris-acetate buffer (TAE) at 25 V for approximately 6 h. After electrophoresis, DNA was visualized by ethidium bromide staining (0.5 μg/mL). The gel was viewed using a UV transilluminator and photographed using Polaroid Polapan 57 film.

DAPI Staining and DNA Content Analysis. At a desired time, untreated and drug-treated cells were harvested by centrifugation, rinsed with phosphate buffered saline (PBS), and fixed on ice for 15 min with 2% paraformaldehyde. After washes with PBS containing 1% FBS, the cells were fixed in 70% alcohol and stored at −20 °C. When all of the samples were collected, they were rinsed with ice-cold PBS supplemented with 10% FBS, stained with DAPI (4′,6-diamino-2-phenylindole) in the dark for 30 min (final concentration 20 μg/mL), washed again, and analyzed by FACS. The blue fluorescence of the DNA-bound DAPI of individual cells was measured with a FACStar Plus Becton Dickinson Immunocytometry System (San Jose, CA).

For morphological examination, 50 μL of cell suspension from each sample was dropped onto a slide, air-dried, mounted with Gel/Mount (Biomeda, Foster City, CA), visualized, and photographed with a Zeiss LSM 310 (Carl Zeiss, Jena, Germany) confocal microscope.

Analysis of Caspase-3 Activity. Intracellular caspase-3 activity was measured using a Caspase-3 Assay Kit (Pharmingen, San Diego, CA) according to the manufacturer's manual as described previously.[29] Briefly, tested and untreated cells were harvested at the indicated times and washed with PBS. Pelleted cells were treated with a lysis buffer provided in the kit (10×10^6 cells/mL). Cell lysate (100 μL) was added to the reaction tubes, one containing 10 μL of reconstituted Ac-DEVD-AMC (caspase-3 fluorogenic substrate) in 1 mL of HEPES buffer and a second with the same amount of Ac-DEVD-AMC and 10 μL of Ac-DEVD-CHO (caspase-3 inhibitor) in 1 mL of HEPES the buffer. Reaction mixtures were incubated for 1 h at 37 °C, and the emitted fluorescence from AMC that was cleaved and released by active caspase-3 was quantified by a UV specrofluorometer (FluoroMax2) with an excitation of 380 nm and an emission of 440 nm.

In Vivo Experiments. HCT-116 human tumor fragments (3 mm × 3 mm) were obtained from donor mice and implanted subcutaneously into the experimental athymic (nu/nuNCr) mice using a tumor implant trocar (Popper and Sons, New Hyde Park, NY). Treatment was initiated 4 days following implantation. Mice were housed in an AAALAC-accredited barrier facility with sterilized chow and hyperchlorinated water provided ad libitum. Tumor growth was monitored using a twice or thrice weekly caliper measurement of the tumor in two dimensions. These measurements were converted to tumor weights using a formula for a prolate ellipsoid: [(length in mm) × (width in mm)^2]/2 = tumor weight (mg).

Acknowledgment. We thank the Structural Biophysics Resource Laboratory, NCI−Frederick for the use of the mass spectrometer. We are grateful to Dr. Dominic Scudiero, Developmental Therapeutics Program, NCI for the NCI 60 cell line assay data and Dr. Sergey Tarasov for the discussions.

Supporting Information Available: Elemental analysis data for the compounds **4ac**, **4ad**, **5ad**, and **6** and NCI 60 human tumor cell line screening data for **4ac** and **4ad**. This material is available free of charge via the Internet at http://pubs.acs.org.

References

(1) Schmitt, C. A.; Lowe, S. W. Apoptosis and therapy. *J. Pathol.* **1999**, *187*, 127−137.
(2) Sen, S.; D'Incalci, M. Apoptosis. Biochemical events and relevance to cancer chemotherapy. *FEBS Lett*. **1992**, *307*, 122−127.
(3) Hannun, Y. A. Apoptosis and the dilemma of cancer chemotherapy. *Blood* **1997**, *89*, 1845−53.

(4) Mesner, P.; Budihardjo, I.; Kaufman, S. H. Chemotherapy-induced apoptosis. *Adv. Pharmacol*. **1997**, *41*, 461−499.
(5) Kamesaki, H. Mechanisms involved in chemotherapy-induced apoptosis and their implications in cancer chemotherapy. *Int. J. Hematol.* **1998**, *68*, 29−43.
(6) Kaufman, S. H.; Earnshaw, W. C. Induction of apoptosis by cancer chemotherapy. *Exp. Cell Res*. **2000**, *256*, 42−49.
(7) Debatin, K.-M. Activation of apoptotic pathways by anticancer treatment. *Toxicol. Lett*. **2000***, 112*−*113*, 41−48.
(8) Nicotera, P.; Leist, M.; Single, B.; Volbracht, C. Execution of apoptosis: converging or diverging pathways? *Biol. Chem*. **1999**, *380*, 1035−1040.
(9) Blagosklonny, M. V. Cell death beyond apoptosis. *Leukemia* **2000**, *14*, 1502−1508.
(10) Formigli, L.; Papucci, L.; Tani, A.; Schiavone, N.; Tempestini, A.; Orlandini, G. E.; Capaccioli, S.; Zecchi Orlandini, S. Aponecrosis: morphological and biochemical exploration of a syncretic process of cell death sharing apoptosis and necrosis. *J. Cell. Physiol*. **2000**, *182*, 41−49.
(11) Cholody, W. M.; Hernandez, L.; Hassner, L.; Scudiero, D. A.; Djurickovic, D. B.; Michejda, C. J. Bisimidazoacridones and Related Compounds: New Antineoplastic Agents with High Selectivity against Colon Tumors. *J. Med. Chem*. **1995**, *38*, 3043−3052.
(12) Hernandez, L.; Cholody, W. M.; Hudson, E. A.; Resau, J. H.; Pauly, G.; Michejda, C. J. Mechanism of Action of Bisimidazoacridones, New Drugs with Potent, Selective Activity against Colon Cancer. *Cancer Res*. **1995**, *55*, 2338−2345.
(13) Turpin, J. A.; Buckheit, Jr. R. W.; Derse, D.; Hollingshead, M.; Williamson, K.; Palamone, C.; Osterling, M. C.; Hill, S. A.; Graham, L.; Schaeffer, C. A.; Bu, M.; Huang, M.; Cholody, W. M.; Michejda, C. J.; Rice, W. G. Inhibition of acute, latent and chronic phase HIV-1 replication by a bistriazoloacridone analogue that selectively inhibits HIV-1 transcription. *Antimicrob. Agents Chemother*. **1998**, *42*, 487−494.
(14) Canellakis, E. S.; Shaw, Y. H.; Hanners, W. E.; Schwartz, R. A. Diacridines: bifunctional intercalators. I. Chemistry, physical chemistry and growth inhibitory properties. *Biochim. Biophys. Acta* **1976**, *418*, 277−289.
(15) Wright, R. G. McR.; Wakelin, L. P. G.; Fieldes, A.; Acheson, R. M.; Waring, M. J. Effects of Ring Substituents and Linker Chains on the Bifunctional Intercalation of Diacridines into Deoxyribonucleic Acid. *Biochemistry* **1980**, *19*, 5825−5836.
(16) Markovits, J.; Garbay-Jaureguiberry, C.; Roques, B. P.; Le Pecq, J.-B. Acridine dimers: influence of the intercalating ring and of the linking-chain nature on the equilibrium and kinetic DNA-binding parameters. *Eur. J. Biochem*. **1989**, *180*, 359−366.
(17) Le Pecq, J.-B.; Le Bret, M.; Barbet, J.; Roques, B. P. DNA polyintercalating drugs: DNA binding of diacridine derivatives. *Proc. Natl. Acad. Sci. U.S.A.* **1975**, *72*, 2915−2919.
(18) Gaugain, B.; Barbet, J.; Oberlin, R.; Roques, B. P.; Le Pecq, J.-B. DNA Bifunctional Intercalators. 1. Synthesis and Conformational Properties of an Ethidium Homodimer and of an Acridine Ethidium Heterodimer. *Biochemistry* **1978**, *17*, 5071−5078.
(19) Tarasov, S. G.; Casas-Finet, J. R.; Cholody, W. M.; Kosakowska-Cholody, T.; Gryczynski, Z. K.; Michejda, C. J. Bisimidazoacridones: 2. Steady-state and time-resolved fluorescence studies of their diverse interactions with DNA. *Photochem. Photobiol.* **2003**, *78*, 313−322.
(20) Segal-Bendirdjian, E.; Coulaud, D.; Roques, B. P.; Le Pecq, J. B. Selective loss of mitochondrial DNA after treatment of cells with ditercalinium (NSE335153), an antitumor bis-intercalating agent. *Cancer Res.* **1988**, *48*, 4982−4992.
(21) Tarasov, S. G.; Casas-Finet, J. R.; Cholody, W. M.; Michejda, C. J. Bisimidazoacridones: Effect of molecular environment on conformation and photophysical properties. *Photochem. Photobiol.* **1999**, *70*, 568−578.
(22) Results from the standard NCI screening can be accessed at the Developmental Therapeutic Program, NCI/NIH web site (http://dtp.nci.nih.gov) with the Search by NSC number option.
(23) Monks, A.; Scudiero, D.; Skehan, P.; Shoemaker, R.; Paull, K.; Vistica, D.; Hose, C.; Langley, J.; Cronise, P.; Vaigro-Wolff, A. Feasibility of a high-flux anticancer drug screen using a diverse panel of cultured human tumor cell lines. *J. Natl. Cancer Inst.* **1991**, *83*, 757−766.
(24) Abad, A.; Gravalos, C.; Font, A.; Molina, F.; Diaz-Puente, M. T.; Fabrega, X.; Benavides, A.; Martin, M. Phase II study of Mitonafide in advanced and relapsed colorectal cancer. *Invest. New Drugs* **1996**, *14*, 223−225.
(25) Casado, A,; Rosell, R.; Garcia-Gomez, R.; Diaz-Rubio, E.; Perez-Manga, G.; Font, A.; Benavides, A.; Martin, M. Phase II study of mitonafide in non-small cell lung cancer (NSCLC). *Invest. New Drugs* **1996**, *14*, 415−417.
(26) Gong, J.; Traganos, F.; Darzynkiewicz. Z. A selective procedure for DNA extraction from apoptotic cells applicable for gel elecrophoresis and flow cytometry. *Anal. Biochem*. **1994**, *218*, 314−319.
(27) Aranha, O.; Gringnon, R.; Fernandes, N.; McDonnell, T. J.; Wood, D. P.; Sarkar, F. Suppression of human prostate cancer cell growth by ciprofloxacin is associated with cell cycle arrest and apoptosis. *Int. J. Oncol.* **2003**, *22*, 787−794.
(28) Cohen, G. M. Caspases: the executioners of apoptosis. *Biochem. J.* **1997**, *326*, 1−16.
(29) Cholody, W. M.; Kosakowska-Cholody, T.; Michejda, C. J. Bisimidazoacridones induce a potent cytostatic effect in colon tumor cells that sensitizes them to killing by UCN-01. *Cancer Chemother. Pharmacol.* **2001**, *47*, 241−249.

JM048946X